Validation of POLDER-2/PARASOL aerosol products over Beijing area

FAN Xue-hua[1,2], CHEN Hong-bin[2], LIN Long-fu[1], HAN Zhi-gang[1], Philippe Goloub[3], ZHANG Wen-xing[2]

1. *Beijing Institute of Applied Meteorology*, *Beijing* 100029, *China*;
2. *Laboratory for Middle Atmosphere and Global Environment Observation*, *Institute of Atmospheric Physics*, *Chinese Academy of Sciences*, *Beijing* 100029, *China*;
3. *Laboratoire d'Optique Atmosphérique*, *Université des Sciences et Technologies de Lille*, *UMR-CNRS* 8518, *Villeneuve d'Ascq*, *Lille* 59655, *France*.

Abstract: This study is devoted to the regional validation of POLDER-2/PARASOL aerosol retrieval scheme over land surfaces against independent automatic sun-photometers located at Beijing and Xianghe sites both included in AERONET (Aerosol Robotic Network)/PHOTONS (PHOtométrie pour le Traitement Opérational de Normalisation Satellitaire). Analysis of the AERONET/PHOTONS volume size distributions shows that the fine mode is very well defined with size-cut of about 0.3μm over Beijing area. POLDER-2/PARASOL aerosol optical thickness (AOT) is shown to be quite consistent with the fine fraction of the size distribution (radius <0.3μm). In other words, POLDER-2/PARASOL retrieval over land is mainly sensitive to the anthropogenic aerosols which are known to have important impacts on the climate, environment as well as human health. However, the Ångström exponent used in the POLDER retrieval algorithm is much higher than the statistic of the AERONET/PHOTONS measurements over Beijing. Thus the derived AOT have been underestimated and the Ångström exponents have been overestimated.

Key words: aerosol, POLDER, PARASOL, volume size distribution, polarized reflectance

CLC number: P407 **Document code**: A

1 INTRODUCTION

Remote sensing of aerosol properties is much more difficult over land than over ocean because of the difficulty in discriminating the aerosol contribution from the ground in top of the atmosphere (TOA) measurements. The problem has been solved in several ways, for example, thermal contrast over desert areas (Legrand *et al.*, 1989), and the reflectance over dense dark vegetation (Kaufman *et al.*, 1997). The new generation of satellite sensor, POLDER (Polarization and Directionality of the Earth's Reflectances) developed by CNES can acquire the global observation of the polarization and directionality of solar radiation reflected by the earth-atmosphere system. The multi-directional, multi-spectral polarization measurements of POLDER provide the new way for the remote sensing of aerosol over land. Ground-based measurements suggest that the polarized light reflected by ground targets is small and stable enough to allow for correction in TOA measurements (Deuzé *et al.*, 1993; Herman *et al.*, 1997). However, atmospheric molecules and most aerosols exhibit rather strong polarization. The aerosol properties could be derived from the measurements of the polarized reflectance by correcting the molecular contribution of TOA signals.

POLDER-1/2 onboard ADEOS-Ⅰ and ADEOS-Ⅱ (Advanced Earth Observation Satellite) spacecrafts are not acquiring data any more because of solar panel failure of the platform. PARASOL (Polarization & Anisotropy of Reflectances for Atmospheric Sciences coupled with Observations from a Lidar) satellite as part of so-called "A-train" carried POLDER-3 instrument for the third time, which affirmed the advantage of multi-directional, multi-spectral polarization measurements and is helpful to better understand the impact of clouds and aerosols on climate. The resolution of POLDER-1/2 is 6km×7km at nadir and the resolution is enhanced to 5km×6 km for PARASOL.

The aerosol operational products including aerosol index, AOT and Ångström exponents are provided by the French POLDER team (Leroy *et al.*, 1997; Deuzé *et al.*, 2001). The preliminary comparison showed that there is a

Received date: 2007-07-06; **Accepted date**: 2007-10-29

Foundation: 973 Program of China under Grant No. 2006CB403702, National Science Foundation of China (40805010), and the French-Chinese Programme de Recherches Avancées (PRAE 04-02).

First-author Biography: FAN Xue-hua (1978—), female. She received the Ph. D degree in atmospheric physics and atmospheric environment in 2007 from the Institute of Atmospheric Physics, Chinese Academy of Science. She is currently a postdoctoral fellow in Beijing Institute of Applied Meteorology. Her research interests include atmospheric radiative transfer modeling and remote sensing of aerosol optical parameters from ground-based and satellite measurements. E-mail: fxh@mail.iap.ac.cn.

general good agreement between ground measurements and POLDER/PARASOL aerosol products over Europe and North America(Goloub & Arino, 2000; Tanré *et al.*, 2001; Vachon *et al.*, 2004). However, there is no work on the validation of POLDER/PARASOL aerosol products around China. The POLDER-2 and PARASOL aerosol products over Beijing area are evaluated based on the AERONET/PHOTONS ground measurements in the paper. The second section briefly recaps the retrieval scheme applied to POLDER/PARASOL reflectances (level 1 data). The third section addresses to the validation dataset over Beijing and Xianghe sites. POLDER-2/PARASOL and AERONET/PHOTONS retrievals are compared and discussed in the fourth section. Conclusions are given in the fifth section.

2 POLDER-2/PARASOL AEROSOL ALGORITHM OVER LAND

According to Deuzé *et al.* (2001) approach developed for POLDER-1/2, one can write the polarized reflectance R_p^{TOA} at top of Atmosphere (TOA), as follows:

$$R_p^{TOA} = R_p^{surf} T + R_{p\_atmos}^{TOA} \quad (1)$$

where R_p^{surf} *and* $R_{p\_atmos}^{TOA}$ are the surface and atmospheric contributions, respectively; T stands for the atmospheric transmittance. The surface polarized reflectance, R_p^{surf}, is modeled using a semi-empirical surface model (Bréon *et al.*, 1995; Nadal & Bréon, 1999) and considered to be spectrally flat.

In the single scattering approximation, the atmospheric contribution $R_{p\_atmos}^{TOA}$ considered for POLDER-1/2 is given by

$$R_{p\_atmos}^{TOA} = \frac{\tilde{\omega}_a \tau_a Q_a(\Theta)}{4\cos\theta_v \cos\theta_s} + \frac{\tau_m Q_m(\Theta)}{4\cos\theta_v \cos\theta_s} \quad (2)$$

where $\tilde{\omega}_a$ is single scattering albedo of aerosols; τ_a and τ_m are respectively aerosol and molecular optical thickness; $Q_a(\Theta)$ and $Q_m(\Theta)$ are the polarized phase functions of aerosol and molecule respectively; θ_s and θ_v are the solar zenith angle and the view zenith angle respectively, whereas Θ is the scattering angle. For PARASOL operational data processing, the pure atmospheric contribution ($R_{p\_atmos}^{TOA}$) is now exactly computed with a radiative transfer code (Deuzé *et al.*, 1989; Vermote *et al.*, 1997).

Downward and upward transmittances are expressed with T factor

$$T = \exp\left(-\left(\frac{\gamma\tau_\lambda^m + \beta\tau_\lambda^a}{\cos\theta_s} + \frac{\gamma\tau_\lambda^m + \beta\tau_\lambda^a}{\cos\theta_v}\right)\right) \quad (3)$$

with γ and β are empirical coefficients (Lafrance *et al.*, 1997); λ is the wavelength.

Aerosol model is described by the single mode lognormal size distribution (with geometric standard deviation, $\sigma = 0.40$ of variance) and various modal radii ranging from 0.05 to 0.15 μm (associated Ångström exponent α ranging from 1.8 to 3.0). The refractive index (m) is $1.47 - 0.01i$ corresponding to small particles absorption. The polarized reflectance R_p^{TOA} at TOA is computed for the given geometry (θ_s, θ_v, Θ), at 670 and 865 nm, a set of 10 aerosol models assumed spherical particles, and a set of increasing AOT to form the LUT. The best agreement (i.e., minimum difference) between computed and measured spectral polarized reflectances provides AOT and the Ångström exponent.

3 POLDER-2/PARASOL AEROSOL PRODUCTS AND VALIDATION DATASET

3.1 POLDER-2/PARASOL aerosol products

POLDER-2/PARASOL aerosol level 2 data consist of AOT at 865 nm (τ_{865nm}^{sat}) and Ångström exponent ($\alpha_{670\_865nm}^{sat}$) retrieval performed on average over 3 × 3 level 1 pixels, thus leading to spatial resolution of about 20km × 20km. For PARASOL, the studied period is from March 2005 to May 2006 and the total number of PARASOL overpass Beijing and Xianghe is 222 days. For POLDER-2, there is less than 7 month data from April 2003 to September 2003 and the total number is 88 days. The overpass time for PARASOL and POLDER-2 is 13:40 and 10:40 respectively.

In the comparison exercise shown in the following section, the central pixel of the satellite is considered located on each sun-photometer site. Moreover, in order to estimate the spatial variability, the standard deviation is computed within a 35km × 35km size area. The temporal match method proposed by Goloub *et al.* (1999) is used in the comparison. The four AOT measurements acquired within ± 30 minutes of the satellite overpass time are selected and averaged. Only days with the ratio of the variance over average AOT (τ_{865nm}^{AER}) less than 0.20 are kept, corresponding to stable atmospheric conditions.

3.2 AERONET/PHOTONS ground-based measurement sites

AERONET/PHOTONS established by NASA and the cooperating institution provided the long-term aerosol data which are fundamental to the estimation of aerosol influence on climate and the ground-based validation of aerosol properties derived from satellite. More than 250 sites are included in the network. CIMEL CE-318 sunphotometers developed by French CIMEL company are used in AERONET/PHOTONS. The direct sun measurements are made at 340, 380, 440, 500, 675, 865, 940 and 1020 nm. These solar extinction measurements are then used to compute AOT at each wavelength except for the 940 nm channel, which is used to retrieve precipitable water in centimeters. The direct sun measurement, almucantar measurement and principal plane measurement are combined to retrieve aerosol size distribution, complex refractive index and single

scattering albedo (Holben *et al.*, 1998). Beijing (Latitude: 39.98° N, Longitude: 116.38° E) became one of long-term sites of AERONET/PHOTONS from April, 2002. Xianghe site (Latitude: 39.75° N, Longitude: 116.96° E) as one of long-term sites of AERONET/PHOTONS from September 2004 is close to Beijing, about 70km southeast from the megacity.

3.3 AERONET/PHOTONS data

3.3.1 *Mean characteristic of AERONET/PHOTONS aerosol size distribution*

The aerosol size distributions over Beijing area are analyzed since the polarization is sensitive to the fine mode particles.

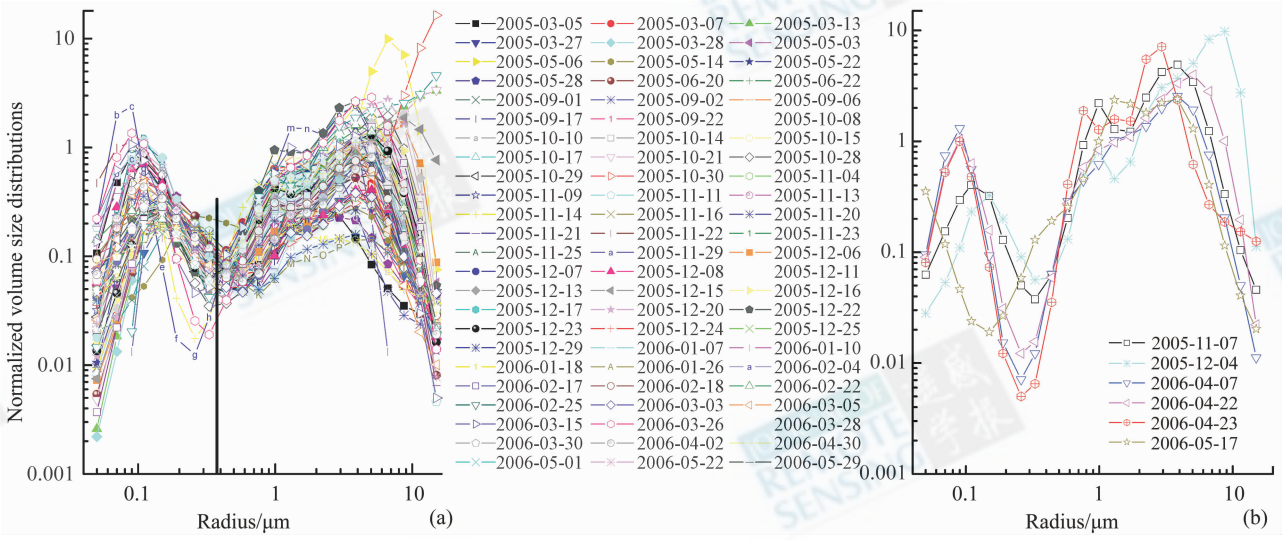

Fig. 1 AERONET/PHOTONS volume size distributions normalized by AOT at 865 nm for $\alpha^{AER}_{670\_865nm} > 0.5$ (a) and $\alpha^{AER}_{670\_865\ nm} \leqslant 0.5$ (b).

Fig. 1 showed the volume size distributions normalized by AERONET/PHOTONS total AOT at 865 nm, *i. e.* $\frac{dV/d\ln r}{\tau^{AER}_{865nm}}$ where V and r stand for volume and particle radius respectively, at Beijing during the whole PARASOL period. Two cases are considered, one with AERONET/PHOTONS Ångström exponent $\alpha^{AER}_{670\_865nm} > 0.5$ accounting for 90% of the dataset (Fig. 1(a)) and the 10% residual situations with $\alpha^{AER}_{670\_865nm} \leqslant 0.5$ dominated by coarse particles (Fig. 1(b)). From Fig. 1, it can be seen that aerosol size distribution is the bimodal mixture of coarse and fine mode particles over Beijing. The fine mode is very well defined with size-cut between 0.3 and 0.4 μm for $\alpha^{AER}_{670\_865nm} > 0.5$ (Fig. 1(a)). The coarse mode amplitude is higher for dust days and the size-cut of the fine mode decreases to 0.2—0.3μm (Fig. 1(b)).

3.3.2 *Recomputation of fine mode (r < 0.3μm) AOT of AERONET/PHOTONS*

The AERONET/PHOTONS fine mode AOT ($r < 0.6$ μm), $\tau^{AER}_{fine(r<0.6\mu m)}$, is systematically larger than AOT retrieved from PARASOL in Beijing because the fine mode threshold around this site is about 0.3μm according to the statistics of size distributions (section 3.3.1). Considering decreasing the fine mode threshold to 0.3μm, the AOT of the particle radius less than 0.3 μm, *i. e.* $\tau^{AER}_{fine(r<0.3\mu m)}$, is recomputed at satellite overpass time.

The first step is to calculate the redefined fine mode ($r < 0.3$μm) AOT from the truncated size distribution and refractive index at sun-photometer inversion time when it is the closest to the satellite overpass time. It is expressed as $\tau^{inv}_{fine(r<0.3\mu m)}$.

The aerosol size distributions of AERONET/PHOTONS are interpolated in the range of 0.05—15μm to truncate at any radius. The fine mode ($r < 0.6$μm) AOTs at 443, 670, 865 and 1020 nm are calculated using Mie code and compared with AERONET/PHOTONS fine mode AOTs $\tau^{AER}_{fine(r<0.6\mu m)}$. The good agreement in Fig. 2 showed the Mie code is reliable.

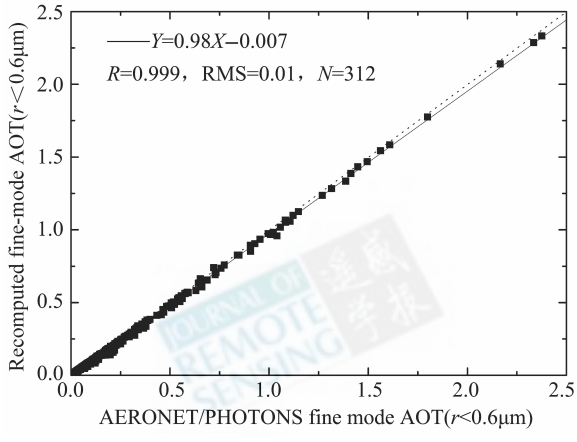

Fig. 2 Comparison between the recomputed fine mode AOT and AERONET/PHOTONS fine mode AOT ($r < 0.6$μm) for 4 wavelengths (443, 670, 865 and 1020 nm).

Accounting to the AOT temporal variation between the inversion time and satellite overpass time, $\tau^{AER}_{fine(r<0.3\mu m)}$ is derived from $\tau^{inv}_{fine(r<0.3\mu m)}$. When the Ångström exponent is rather constant, $\tau^{AER}_{fine(r<0.3\mu m)}$ can be estimated from $\tau^{inv}_{fine(r<0.3\mu m)}$ using the relation as follows

$$\tau^{AER}_{fine(r<0.3\mu m)} = \tau^{inv}_{fine(r<0.3\mu m)} \times \left(\frac{\tau^{AER}_{865nm}}{\tau^{inv}_{865nm}}\right) \quad (4)$$

where τ^{AER}_{865nm} is the total AOT selected and averaged using the four measurements within ± 30 minutes of the satellite overpass time and τ^{inv}_{865nm} is total AOT measured at inversion time.

Second, the stability of the Ångström exponent $\alpha^{AER}_{670\_865nm}$ is checked between the sun-photometer inversion time and satellite overpass time. According to the statistics, the days with the absolute difference of $\alpha^{AER}_{670\_865nm}$ between the two times less than 0.1 account for more than 80% of the total samples in Beijing and Xianghe. So, the days with the absolute difference of $\alpha^{AER}_{670\_865nm}$ more than 0.1 are rejected because the correction as in formula (4) cannot be used under this condition. Thus, the estimated fine mode ($r<0.3\mu m$) AOT at satellite overpass time is acquired according to the Eq. (4). Then, the fine mode Ångström exponents are derived from fine mode AOT.

3.3.3 Cloud screening

The acquired real time AERONET/PHOTONS data is level 1.0 and level 1.5. The level 1.0 data are used because there are not enough level 1.5 samples and the automatically cloud screening of level 1.5 data rejects some interesting events such as variable aerosol plumes, dust(Smirnov *et al.*, 2000). Thus, the cloud filtering must be done. Several methods are combined to eliminate the cloud contamination. First, the almucantar and principal plane data are carefully inspected. The sky radiance scanning about the solar disk should be symmetric and smooth when it is cloudless and homogenous. Second, the weather records in Beijing and the whole sky imager in Xianghe are used. The ancillary information helps to keep the reliable data to compare between satellite and ground measurements. After all screening and processing are applied, the numbers of the matched samples between the satellite and ground-based measurements for POLDER-2 and PARASOL period in Beijing and Xianghe are given in table 1.

Table 1 Matched number of satellite retrieval and ground-based measurements

Site \ Period	POLDER-2/ADEOS-Ⅱ (Apr., 2003—Sep., 2004)	PARASOL (Mar., 2005—May., 2006)
Beijing (39.98°N, 116.38°E)	18	78
Xianghe (39.75°N, 116.96°E)	0	70

4 COMPARISON OF SATELLITE AND GROUND-BASED MEASUREMENTS

4.1 Time series of fine mode AOT

Fig. 3 shows the time series of POLDER-2/PARASOL AOT τ^{sat}_{865nm} and recomputed fine mode AOT $\tau^{AER}_{fine(r\leq0.3\mu m)}$ of AERONET/PHOTONS at 865 nm in the two sites. Fig. 3(a) is for Beijing POLDER-2 period, Fig. 3(b) is the same as Fig. 3(a) except for PARASOL period and Fig. 3(c) is for Xianghe PARASOL period.

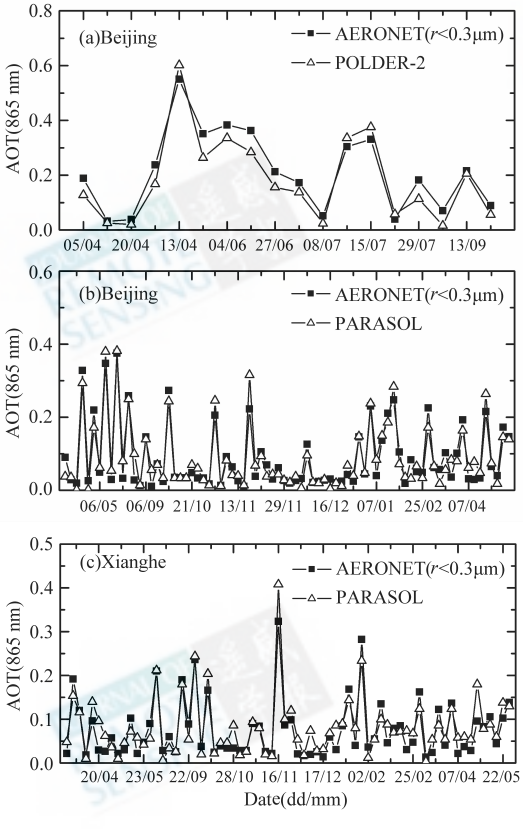

Fig. 3 Day to day variation of AOT at 865 nm during the validation period of POLDER-2 in Beijing(a), PARASOL in Beijing (b), and PARASOL in Xianghe (c), compared with AERONET/PHOTONS recomputed fine mode AOT.

Taking Beijing PARASOL period for example, there are some days with very high AOT. Table 2 lists AERONET/PHOTONS total and fine mode AOT, as well as Ångström exponent plus PARASOL retrieved AOT and Air Pollution Index (API) (The maximum of the three kinds of pollution indices is defined as API for the day, i.e., API = MAX(PM_{10}, SO_2, NO_2). The pollutant with the largest pollution index is regarded as the chief pollutant. (http://www.sepa.gov.cn/quality/airforecast/air_forecast.php).). These data correspond to high fine mode AOT, i.e., both $\tau^{AER}_{fine(r<0.3\mu m)}$ and τ^{sat}_{865nm}

are greater than 0.2; additionally, a dust storm day 2006-05-17 is also included in the table. The major pollutants of all the days are PM_{10}. The API is greater than 300 and the pollution is heavy on 2005-11-04 and 2006-05-17. However, the AOT is different for the two days. The fine mode AOT accounts for 41% of total AOT and $\alpha^{AER}_{670\_865nm}$ is 1.04 on 2005-11-04 which illustrates the aerosols are mixture of fine and coarse mode. The $\alpha^{AER}_{670\_865nm}$ is only 0.06 and the total AOT at 865 nm reaches up to 1.43, but the fine mode AOT is less than 0.05 on 2006-05-17. In addition, PARASOL AOT is only 0.02 which exhibits aerosols are mainly composed of dust particles on that day. Some days with high AOT are not corresponding to the high daily PM_{10} concentrations because PM_{10} concentration include those under all-sky conditions and throughout the whole day when AOT is available only in the daytime and under clear-sky conditions. Moreover, PARASOL AOT is made up of mostly fine particles, so PM_{10} is not the optimal indicator of AOT (Xia *et al.*, 2005).

Table 2 The information of the days with high fine mode AOT and a dust storm day

Date yy-mm-dd	$\tau^{AER}_{865\ nm}$	$\tau^{ARE}_{fine(r<0.3\mu m)}$	$\alpha^{AER}_{670\_865nm}$	τ^{sat}_{865nm}	Major Pollutant	API
2005-03-27	0.67	0.33	1.36	0.29	P_{M10}	161
2005-05-14	1.64	0.35	0.88	0.38	P_{M10}	85
2005-05-28	0.77	0.38	1.43	0.38	P_{M10}	120
2005-06-22	0.52	0.26	1.41	0.25	P_{M10}	116
2005-10-10	0.52	0.29	1.42	0.25	P_{M10}	167
2005-04-11	0.51	0.21	1.04	0.25	P_{M10}	330
2005-11-16	0.48	0.22	1.36	0.32	P_{M10}	104
2005-12-29	0.51	0.23	1.16	0.24	P_{M10}	113
2006-01-26	0.54	0.25	1.24	0.28	P_{M10}	157
2006-04-30	0.92	0.22	0.74	0.26	P_{M10}	165
2006-05-17	1.43	0.04	0.06	0.02	P_{M10}	500

From individual size distribution for Beijing and Xianghe, the fine mode fraction corresponding to radius less than 0.3 μm, $C_{fine(r<0.3\mu m)} = \frac{\tau^{AER}_{fine(r<0.3\mu m)}}{\tau^{AER}_{total}}$ is computed. The averaged fine mode fraction during the validation period $\overline{C_{fine(r<0.3\mu m)}}$ is 0.30 ± 0.12 and 0.31 ± 0.13 respectively for Beijing and Xianghe. The POLDER-2/PARASOL AOTs are divided by the averaged fine mode fractions in the two sites to estimate the total AOT τ^{est}_{total} (the superscript "est" stands for estimation). The time series of the total AOT estimated and AERONET/PHOTONS total AOT are showed in Fig. 4. Fig. 4 (a) is for POLDER-2/ADEOS-Ⅱ period of Beijing, Fig. 4 (b) is for PARASOL period of Beijing and Fig. 4 (c) is for PARASOL period of Xianghe. There is a good agreement between the estimation and AERONET/PHOTONS. The correlative coefficients are 0.91, 0.99 and 0.80 for the three situations as shown in Fig. 6; the root mean squares are 0.133, 0.165 and 0.133 respectively. However, the total AOT is overestimated due to the fine mode fraction underestimated for heavy pollution of fine particles (for example, 2005-11-04 and 2005-11-16); the total AOT is underestimated due to the fine mode fraction overestimated for heavy pollution of coarse particles (for example, 2006-05-17).

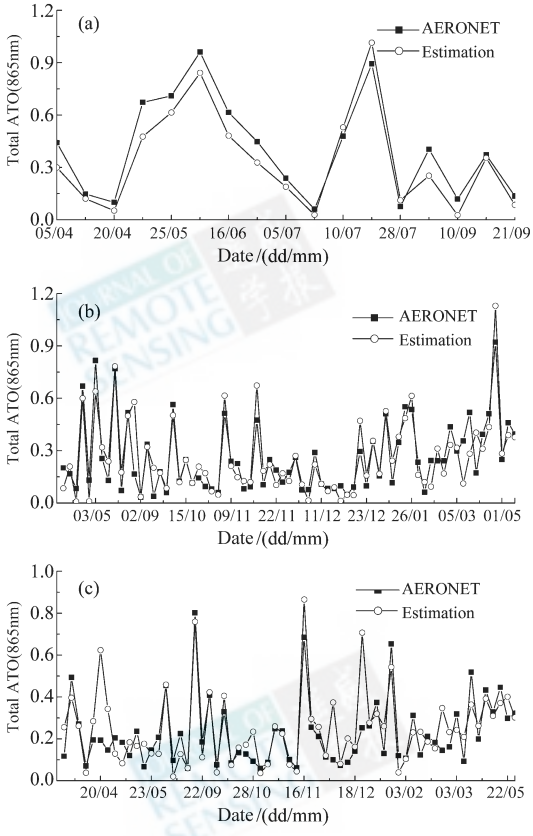

Fig. 4 Day to day variation of total AOT estimated from τ^{sat}_{865nm} and $\overline{C_{fine(r<0.3\mu m)}}$ at 865 nm during the validation period of POLDER-2 in Beijing (a), PARASOL in Beijing (b), and PARASOL in Xianghe (c), compared with AERONET/PHOTONS total AOT.

4.2 Comparison of aerosol optical properties between satellite and ground-based measurements

The comparisons of POLDER-2/PARASOL AOT and AERONET/PHOTONS fine mode AOT ($r < 0.3\mu m$) are showed in Fig. 5(a) for Beijing and in Fig. 5(c) for Xianghe. The comparisons of fine mode Ångström exponents between POLDER-2/PARASOL and ground-based measurements are showed in Fig. 5(b) for Beijing and in Fig. 5(d) for Xianghe. The error bars on the X-axis are the errors of recomputed fine AOT from AERONET/PHOTONS, which is defined as the following:

$$\varepsilon = \frac{\left|\tau_{cal}^{total} - \tau_{mea}^{total}\right|}{\tau_{cal}^{total}} \times \tau_{cal}^{fine} \quad (5)$$

where the subscripts "cal" and "mea" denote the calculations and measurements respectively; the superscripts "total" and "fine" denote the total AOT and fine mode AOT. Because the computed total AOT, τ_{cal}^{total}, and the measured total AOT, τ_{mea}^{total}, are very close, ε is very small so that the error bars on the X-axis are almost invisible. The error bars of Y-axis represent the spatial deviation computed over the 35km × 35km size window for POLDER-2/PARASOL.

There is a general good agreement between AERONET/PHOTONS fine mode AOT and PARASOL level 2 AOT, as shown in Fig. 5(a) and(c), whether in Beijing or in Xianghe. The correlation coefficients are respectively 0.95 and 0.90 for Beijing and Xianghe. The slopes are very close to 1. Equivalent results (correlation coefficient of 0.95, slope of 1.04) are found for Beijing with POLDER-2.

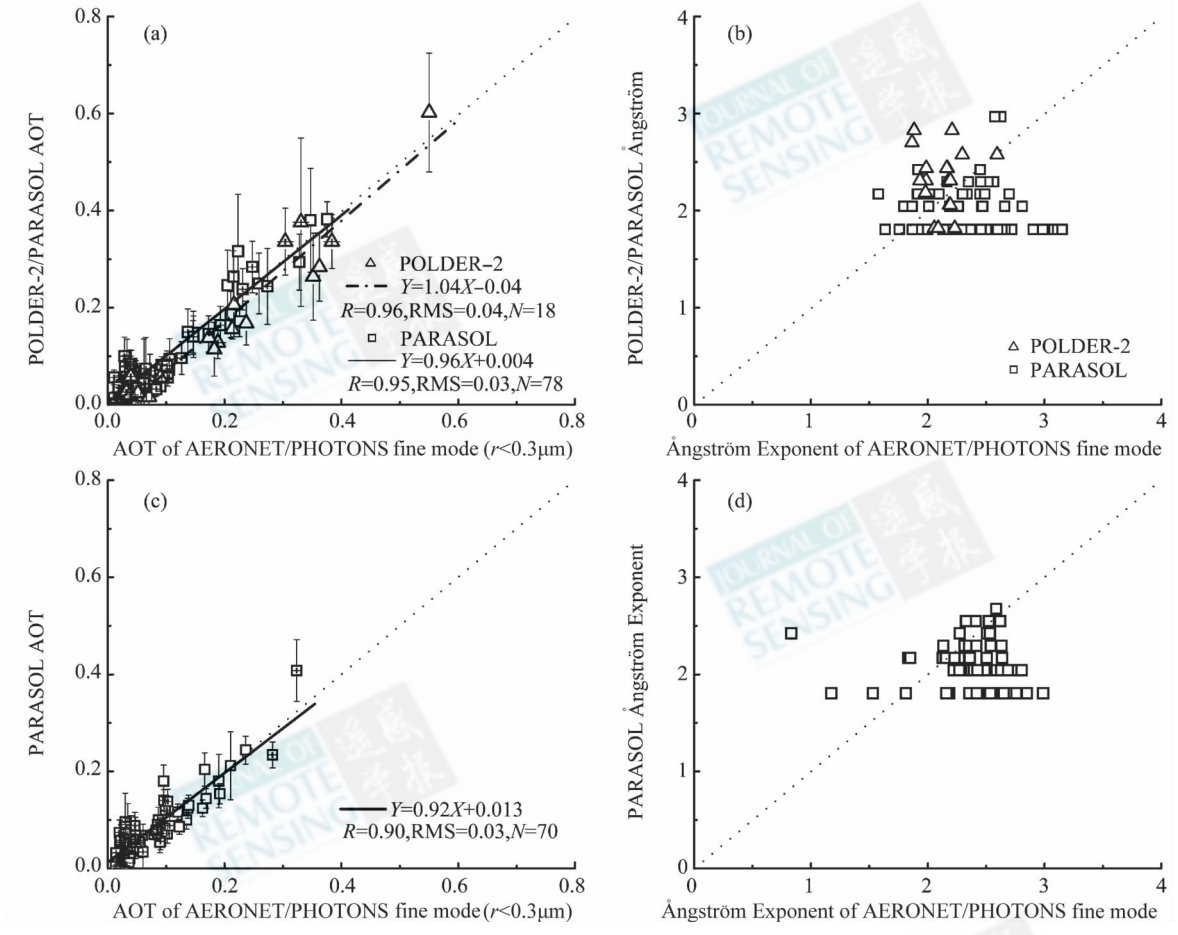

Fig. 5 POLDER-2/PARASOL AOT and Ångström exponent versus those of AERONET/PHOTONS fine mode for Beijing(a),(b) and Xianghe(c),(d)

There are large standard deviations on satellite axis for some days, especially on the days with very low AOT and high AOT. For the days with low AOT, the high standard deviation may be explained by the spatial variation of the surface polarization since the surface contribution is relatively more important in these conditions. In cases of high AOT, Beijing site during PARASOL period was considered. In Fig. 5(a), there are four days with large error bar 2005-05-14 (0.11), 2005-10-10 (0.08), 2005-11-04 (0.07), and 2005-11-16 (0.12). The values in the brackets are standard deviations for the corresponding day. There was strong daily variation of AOT and $\alpha_{670\_865nm}^{AER}$ was 0.88 on 2005-05-14, which implies the atmosphere was not spatially homogeneous.

According to weather report, that day was partly cloudy. The atmosphere was a little hazy on 2005-10-10 according to the weather record and there was small pollution (Table 1) with $\alpha^{AER}_{670\_865nm}$ around 1.42. The pollution was dominated by fine mode aerosols from local emission according to the back trajectory (http://aeronet.gsfc.nasa.gov) so the spatial deviation is large. The high standard deviations on 2005-11-04 and 2005-11-16 can be explained with the same reason; the local pollution on 2005-11-04 was heavier than two other days.

For Ångström exponent, there are 49 cases with the value 1.806 for Beijing PARASOL period (Fig. 5(b)), which is more than 60% of the total 78 days. This value corresponds to the lowest value considered in the set of 10 aerosols model. The statistical averaged Ångström exponent for 4-year AERONET/PHOTONS data over Beijing is about 1.2 (Fan *et al.*, 2006). It is obvious that the Ångström exponents ranging from 1.8 to 3.0 are overestimated around Beijing area. The aerosol model considering the effective radius and effective variance is more reasonable in Beijing region.

The scattering plot of the total AOT estimated τ^{est}_{total} and AERONET/PHOTONS total AOT τ^{AER}_{total} for Ångström exponent higher than 0.5 are showed in Fig. 6(a) for Beijing and in Fig. 6(b) for Xianghe. The correlation coefficients between them are higher than 0.8 and the slopes are close to 1 over Beijing and Xianghe sites.

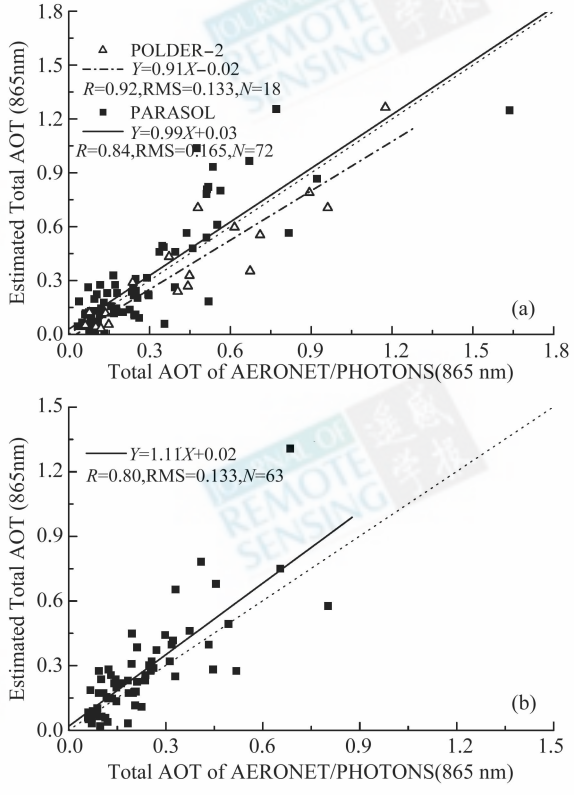

Fig. 6 POLDER-2/PARASOL total AOT computed from τ^{sat}_{865nm} and $C_{fine(r<0.3\mu m)}$ versus those of AERONET/PHOTONS for Beijing (a) and Xianghe (b) in case of $\alpha^{AER}_{670\_865nm}>0.5$.

Dust events release much non-spherical coarse particles. The departure from sphericity tends generally to lower the polarized light scattered by the particles (Cai & Liu, 1982; Mishchenko & Travis, 1994). Thus, the spherical models used in the retrieval will lead to overestimate the polarized light in the presence of non-spherical particles and underestimate the AOT. Moreover, polarization at side scattering angles is mainly generated by very small particles (Hansen & Travis, 1974). The polarization of dust particles is typically 5 to 10 times lower than that of fine particles. The single mode lognormal size distribution did not consider the relationship between large/nonpolarizing and small/polarizing particles (Deuzé *et al.*, 2001). Therefore there is the bias in the AOT retrieval on dust days.

5 CONCLUSIONS

At the regional scale, the contribution of urban/industrial aerosols appears significant in China (Tanré, *et al.*, 2001; Qian & Giorgi, 2000). The analysis on AERONET/PHOTONS size distribution exhibits the size-cut of fine mode is about 0.3 μm over Beijing area. The comparison shows the aerosol products of POLDER-2/PARASOL are sensitive to the accumulation mode ($r<0.3\mu m$) aerosols mainly coming from anthropogenic sources. It is helpful to separate the pollution and dust sources and investigate the local emission and transport of pollutants over the land.

On the other hand, the Ångström exponents ranging from 1.8 to 3.0 in the aerosol model of POLDER operational algorithm are overestimated over Beijing area, which results in the limitation that fine-mode aerosols are dominant and AOT is underestimated.

The total AOTs for the two sites are estimated from POLDER-2/PARASOL AOT τ^{sat}_{865nm} and the averaged fine mode fraction $\overline{C_{fine(r<0.3\mu m)}}$. The total AOT estimated and the AERONET/PHOTONS total AOT are close. The correlation coefficients are above 0.8 and the slopes are very close to 1. The method is usable to estimate the AOT roughly.

Acknowledgements The authors would like to thank the LOA and ICARE center for processing the POLDER/PARASOL level 2 data used in this study. A great thanks is also to the Xianghe observation of IAP, CAS for the total sky image data.

REFERENCES

Bréon F M, Tanré D, Leconte P, *et al.* 1995. Polarized reflectance of bare soils and vegetation: measurements and models. *IEEE Trans. Geosci. Remote Sens.* **33**:487—499

Cai Q M, Liu K N. 1982. Polarized light scattering by hexagonal ice

crystals: theory. *Applied Optics*, **21**(19):3569—3580

Deuzé J L, Bréon F M, Deschamps P Y, *et al.* 1993. Analysis of the POLDER (Polarization and Directionality of the Earth's Reflectances) airborne instrument observations over land surfaces. *Remote Sens. Environ*, **45**:137—154

Deuzé J L, Bréon F M, Devaux C, *et al.* 2001. Remote sensing of aerosols over land surfaces from POLDER-ADEOS-1 polarized measurements. *J. Geophys. Res*, **106**:4913—4926

Deuzé J L, Herman M, Santer R. 1989. Fourier series expansion of the transfer equation in the atmosphere-ocean system. *J. Quant. Spectrosc. Radiat. Transfer*, **41**:483—494

Goloub P, Tanré D, Deuzé J L, *et al.* 1999. Validation of the first algorithm applied for deriving the aerosol properties over the ocean using the POLDER/ADEOS measurements. *IEEE Trans. Geosci. Remote Sens*, **37**(3):1586—1596

Goloub P, Arino O. 2000. Verification of the consistency of POLDER aerosol index over land with ATSR-2/ERS-2 fire Product. *Geophysical Research Letters*, **27**(6): 899—902

Hansen J E, Travis L D. 1974. Light scattering in planetary atmospheres. *Space Science Reviews*, **16**:527—610

Herman M, Deuzé J L, Devaux C, *et al.* 1997. Remote sensing of aerosols over land surfaces including polarization measurements and application to POLDER measurements. *J. Geophys. Res*, **102**(D14):17039—17049

Holben B N, Eck T F, Slutsker I, *et al.* 1998. AERONET-A federated instrument network and data archive for aerosol characterization. *Rem. Sens. Environ*, **66**:1—16

Kaufman Y J, Tanré D, Remer L A, *et al.* 1997. Operational remote sensing of tropospheric aerosol over land from EOS-Moderate resolution imaging spectroradiometer. *J. Geophys. Res*, **102**: 17051—17067

Legrand M, Bertrand J J, Desbois M, *et al.* 1989. The potential of infrared satellite data for the retrieval of saharan-dust optical depth over africa. *J. Applied Meteo*, **28**(4):309—318

Leroy M, Deuzé J L, Bréon F M, *et al.* 1997. Retrieval of atmospheric properties and surface bi-directional reflectances over land from POLDER/ADEOS. *J. Geophys. Res*, **102** (D14): 17023—17037

Mishchenko M I, Travis L D. 1994. Light scattering by polydispersions of randomly oriented spheroids with sizes comparable to wavelengths of observation. *Applied Optics*, 33:7206—7225

Nadal F, Bréon F M. 1999. Parameterization of surface polarized reflectances derived from POLDER spaceborne measurements. *IEEE Trans. Geosci. Remote Sens.* **37**:1709—1719

Qian Y, Giorgi F. 2000. Regional climatic effects of anthropogenic aerosols? The case of southwestern China. *Geophys. Res. Lett*, **27**(21):3521—3524

Smirnov A, Holben B N, Eck T F, *et al.* 2000. Cloud screening and quality control algorithms for the AERONET database. *Remote Sens. Environ*, **73**:337—349

Tanré D, Bréon F M, Deuze J L, *et al.* 2001. Global observation of anthropogenic aerosols from satellite. *Geophysical Research Letters*, **28**(24):4555—4558

Vachon F, Royer A, Aubé M, *et al.* 2004. Remote sensing of aerosols over north American land surfaces from POLDER and MODIS measurements. *Atmospheric Environment*, **38**:3501—3515

Vermote E F, Tanré D, Deuzé J L, *et al.* 1997. Second simulation of the satellite signal in the solar spectrum, 6S: An overview. *IEEE Trans. Geosci. Remote Sens*, **35**:675—686

Xia X A, Chen H B, Wang P C, *et al.* 2005. Aerosol properties and their spatial and temporal variations over north China in spring 2001. *Tellus.* Ser. B. **57**:28—39

POLDER-2/PARASOL 卫星气溶胶业务产品在北京地区的验证分析

范学花[1,2],陈洪滨[2],林龙福[1],韩志刚[1],Philippe Goloub[3],章文星[2]

1. 北京应用气象研究所,北京 100029;
2. 中国科学院大气物理研究所中层大气与全球环境探测实验室,北京 100029;
3. Laboratoire d'Optique Atmosphérique, Université des Sciences et Technologies de Lille 59655,法国

摘 要: 利用地面 AERONET/PHOTONS 气溶胶观测网北京和香河站点的资料,在北京地区对 POLDER-2/PARASOL 卫星多角度偏振信息获得的气溶胶反演产品进行了验证分析。地基 AERONET/PHOTONS 观测网的体积谱分布资料分析显示,在北京地区气溶胶尺度分布的细粒子截断半径约为 0.3μm。将 POLDER-2/PARASOL 卫星气溶胶业务产品和重新定义的地基 AERONET/PHOTONS 细模态(半径 $r<0.3\mu m$)气溶胶光学厚度(AOT)比较,两者在北京地区有着很好的一致性,说明卫星的气溶胶业务反演产品表征了主要来自人类污染排放的细粒子气溶胶贡献。然而,由于 POLDER 系列卫星业务反演方法固定了埃斯屈朗(Ångström)指数的变化范围是 1.8 ~ 3.0,造成了细粒子贡献占绝对主导的局限。由地基 AERONET/PHOTONS 观测资料的分析可知,这个埃斯屈朗指数的先验值远远大于北京地区的地基测量结果,导致了 POLDER 业务反演的气溶胶光学厚度偏低,埃斯屈朗指数偏高。

关键词: 气溶胶,POLDER,PARASOL,体积谱分布,偏振反射率